

Two-Dimensional Condensation of DNA Molecules on Cationic Lipid Membranes

Ye Fang and Jie Yang*

Physics Department, University of Vermont, Cook Building, Burlington, Vermont 05405

Received: August 6, 1996; In Final Form: October 8, 1996[⊗]

DNA molecules adsorbed onto supported cationic lipid membranes are highly condensed. The 2-D condensation requires the presence of free DNA molecules in the solution for a period about 12 h, in which the ratio of adsorbed DNA to the free DNA is about 5% or less. Once condensed, the adsorbed DNA molecules remain on the membrane after removing free DNA molecules in the solution. The adsorption–condensation of both the linear and the circular forms of DNA onto the cationic membrane is independent of the length of DNA. For the condensed DNA, the interhelical distance increases with increase in the concentration of monovalent Na^+ ions. The fluidity of the membrane is essential to induce the close packing of the adsorbed DNA. Possible mechanisms of our findings are discussed.

Introduction

The condensation of DNA has been shown to promote increasing activities in various biological processes, including gene recombination and strand exchange,^{1–4} DNA polymerization and ligation,^{5,6} catenation of circular plasmid DNA,⁷ and replication.^{8–10} It is therefore of great importance to study *in vitro* DNA condensation for the understanding of the molecular level details of the above biological processes. It has been shown that DNA molecules condense into various ordered phases at high concentrations in aqueous solutions.^{11–15} Furthermore, an extensively studied phenomenon is that DNA molecules condense into toroids or rods in the presence of polyvalent cations, such as spermine, spermidine, Mn^{2+} , and $\text{Co}^{3+}(\text{NH}_3)_6$.^{7,16–29} These phenomena demonstrate that the condensation of DNA generates rich structures which are of interest and importance not only for their structural characteristics and molecular organizations but also for their possible roles in promoting the aforementioned biological activities.

The polyvalent-ion-induced DNA condensation involves delicate energetics of the ions and DNA, with ions screening the long-range electrostatic intra- and inter-DNA interactions.^{17,30} These phenomena are three-dimensional in nature in which DNA molecules have high degrees of freedom. For systems of a reduced dimensionality, the phenomena of DNA condensation may be of a different nature. Here, we report experimental results of structural studies of DNA adsorbed and condensed onto two-dimensional cationic lipid membranes using atomic force microscopy (AFM) in solution.

The AFM is a newly developed surface structure probing instrument,³¹ and its capability of operating in solution has opened a new avenue in determining the structure of biological specimens at high resolution in physiologically relevant conditions.^{32–38} The power of the instrument in biological applications has been demonstrated by recent reports on the resolution of the pitch of DNA in solution,^{39,40} on high-resolution imaging of soluble and membrane proteins in solution,^{38,41–47} and on structural studies of model membranes.^{46,48–52} Therefore, AFM is suitable for studies of the molecular level structure of DNA in solution. Our results show that DNA molecules are highly condensed when adsorbed onto two-dimensional supported membranes of cationic lipids, dipalmitoyldimethylammoniumylpropane (DPDAP) and distearoyldimethylammo-

niumylpropane (DSDAP). The DPDAP has a broad main phase transition ($T_m \sim 29^\circ\text{C}$), and DNA molecules adsorbed onto which are closely packed. The DSDAP has a sharp main phase transition ($T_m \sim 38^\circ\text{C}$) on which adsorbed DNA molecules show an apparent decrease in the interhelical distances after heating the membranes to pass the main phase transition. These results suggest the existence of a DNA–DNA attraction that facilitates the condensation of adsorbed DNA molecules on the 2-D membranes. Furthermore, the condensation of DNA onto the 2-D membranes is independent of the length of DNA and disregards whether the DNA molecules are circular or linear. Possible mechanisms and some biological implications are discussed.

Experimental Section

Materials. Cationic lipids (DPDAP and DSDAP) in powder form were purchased from Avanti Polar Lipids (Alabaster, AL) and used without further purification. All DNA molecules were obtained from Sigma (St. Louis, MO) and used after appropriate dilution. The DNA molecules include Col E1 plasmid DNA of about 6600 bp, pTZ plasmid DNA of 2880 bp, λ -DNA, and a DNA marker pUC 18 Hae III digest.

Specimen Preparation. Supported unilamellar bilayers of cationic lipids were prepared with the vesicle fusion method.^{47,48} Briefly, a glass culture tube was used to contain about 1 mL of a lipid suspension at a concentration about 0.25 mg/mL in 20 mM NaCl. The tube was then sonicated until clear under nitrogen gas,^{53,54} using a Fisher FS3 ultrasonic cleaner. Afterward, a droplet ($\sim 200\ \mu\text{L}$) of the lipid suspension was applied to cover a piece of freshly cleaved mica. The substrate was then store at 4°C . Usually, the incubation time for DPDAP is about 24 h and that for DSDAP is about 36 h. Finally, the substrate was heated at 50°C for about 1 h. The existence and the quality of the bilayer were examined by AFM. For supported bilayers of large surface coverage without excessive aggregates, DNA was then allowed to incubate with the bilayers at 4°C overnight. The typical concentration of DNA in the incubation is $1\ \mu\text{g/mL}$ or higher in a droplet of about $200\ \mu\text{L}$. For the DNA concentration lower than $1\ \mu\text{g/mL}$, we usually do not observe stably adsorbed DNA molecules on the cationic lipid bilayers for all kinds of DNA molecules used in this study. Before imaging, the substrate was washed to remove free DNA molecules in the droplet.

DSC. Cationic lipid powder was suspended in 20 mM NaCl, 5.4 mg/mL for DPDAP and 5 mg/mL for DSDAP. The sample

[⊗] Abstract published in *Advance ACS Abstracts*, December 15, 1996.

was loaded to a DSC cell of a volume of 75 μL . DSC scans were carried out at a constant rate of 0.2 $^{\circ}\text{C}/\text{min}$, with a DSC-7 from the Perkin-Elmer (Norwalk, CT).

Langmuir Trough. A Nima Langmuir trough was used. Lipids were dissolved in chloroform at 1 mg/mL, and spread on the air/water interface. Calibrated micropipets were used to spread the lipids on the monolayer. A period of about 20 min was allowed for solvent evaporation before obtaining the area–pressure curve.

Atomic Force Microscopy. A NanoScope E AFM and oxide-sharpened Si_3N_4 tips with a nominal spring constant of 0.06 N/m, all from Digital Instruments, were used in this work. AFM images were obtained in the contact mode under a probe force of 0.1–0.2 nN, at a pixel number of 512×512 , and with a scanning line speed of 5 Hz. For imaging at 9 $^{\circ}\text{C}$, the AFM head unit is housed in a sealed chamber made of copper. The wall of the chamber is surrounded by copper tubing, in which coolant was circulated to regulate the interior temperature. Several hours waiting was needed in order to settle down instrumental drift at the controlled temperature. A rubber glove is installed at the top of the chamber to facilitate adjustments of detector position. A window is also installed to allow visual guidance of necessary adjustments.

Results

Cationic Lipid Membranes. Vesicles or aggregates composed of cationic lipids have been used to facilitate gene transfer and DNA delivery in various systems.^{55,56} The lipids we used have some interesting features. For our purpose, we need to characterize the structure of supported bilayers made of the cationic lipids, DPDAP and DSDAP. Supported bilayers made of these lipids are planar, containing some defects for most specimens. Figure 1 shows two examples. The thickness of these bilayers is about 5 nm, without any apparent difference for the two lipids. We note that this thickness is about 1 nm thinner than the corresponding phosphatidylcholine (PC) bilayers of the same acyl chain lengths.^{48,50} The fact that the thickness is thinner by 1 nm suggests a thinner hydration layer between the bilayer and the substrate.^{57,58} The average molecular area of the cationic lipids is smaller (see below) than that of the PC lipids.

The phase behavior for the two lipids has some unique features. Figure 2 shows two curves of the two lipids by differential scanning calorimetry (DSC). The DPDAP has a broad main phase transition, with the peak temperature at about 29 $^{\circ}\text{C}$. The DSDAP has a sharp main phase transition (peaked at about 38 $^{\circ}\text{C}$), as normally observed in phospholipids.⁵⁹ The transition enthalpies for DPDAP and DSDAP are 13 and 15 kcal/mol, respectively, much larger than those in PC bilayers of the same acyl chain lengths (8.7 and 11 kcal/mol for DPPC and DSPC, respectively).⁵⁹

The molecular surface area of the lipids in bilayers can be estimated from the area–pressure curve while spreading lipid monolayers on an air–water interface. The area–pressure curves for both DPDAP and DSDAP, obtained on a Langmuir trough, are shown in Figure 3. These lipids have a collapse surface pressure of ~ 55 mN/m. It has been known that the natural surface pressure of typical biological membranes corresponds to a monolayer pressure of about 50 mN/m.⁶⁰ On this basis, we estimate the molecular surface areas for both DPDAP and DSDAP to be about 37 and 40 $\text{\AA}^2/\text{lipid}$, respectively. Assuming one positive charge per headgroup, the surface charge density for the two cationic lipid bilayers is about 4×10^{-5} C/cm². This value is of the same order of the charge densities for electrodes in electrochemical interfaces.⁶¹ Therefore, if the

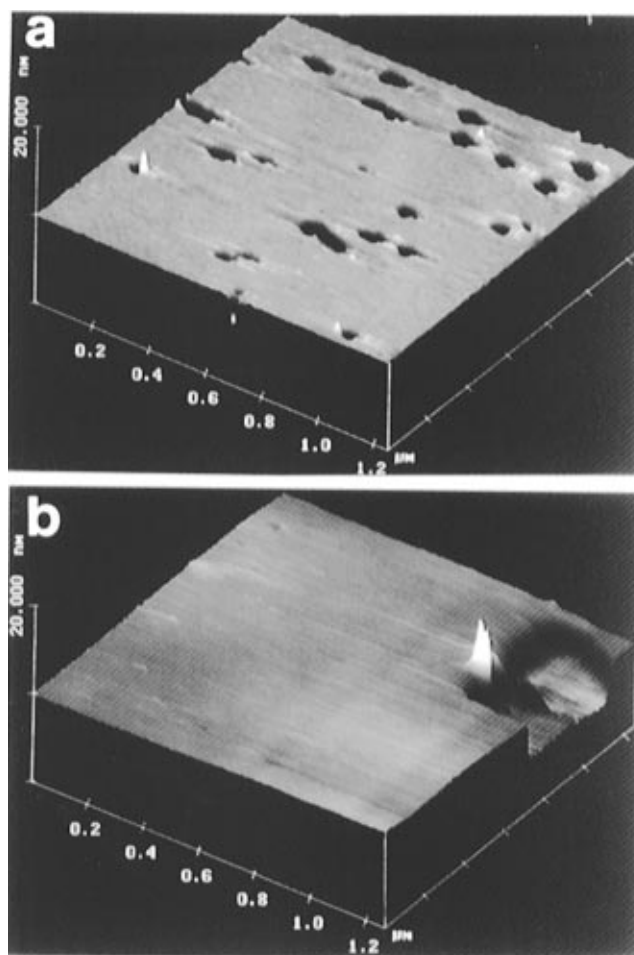


Figure 1. Two supported bilayers of cationic lipids in 20 mM NaCl. The existence of some defects proves the existence of planar bilayer on the mica substrate, in which (a) is a bilayer of DPDAP and (b) is a bilayer of DSDAP. The thickness of both bilayers is about 5 nm.

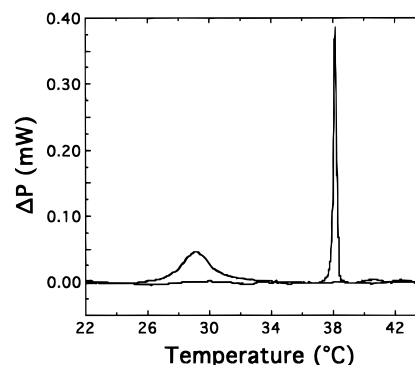


Figure 2. Two profiles from DSC studies of cationic lipids. The one with a broad transition belongs to DPDAP, and the other one belongs to DSDAP.

screening effect is not sufficiently strong, the electrostatic interaction between the cationic lipid bilayers and acidic DNA molecules in solution should draw the DNA molecules to the bilayers.

Close-Packing of DNA on DPDAP. On 2-D cationic lipid bilayer membranes, the concentration of adsorbed DNA is much higher than that in the incubation solution. However, the total amount of DNA on the membrane is only about 5% of the total DNA molecules initially in the incubation droplet. The structure of DNA on cationic lipid membranes indicates that the phenomenon is not just a simple adsorption because of the electrostatic attraction between opposite charges of the DNA and the lipids. In almost all AFM images, we have seldom

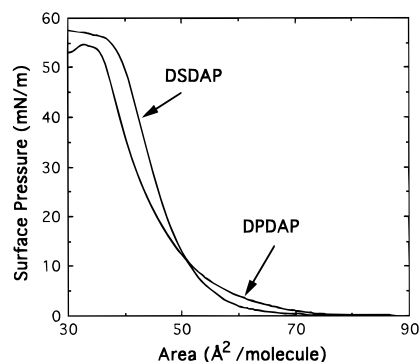


Figure 3. Two area–pressure curves of the cationic lipids obtained by a Langmuir trough. Each curve was obtained by averaging three independent runs.

observed DNA segments crossing each other. The crossing should be a common structure for simple adsorption, since statistically it bares more weight than parallel arrangement of DNA segments. Thus, the DNA on the cationic lipid membranes is a condensation phenomenon associated also with a dimensionality reduction. On the other hand, adsorbed DNA molecules remain condensed on the cationic lipid membranes, after removing free DNA molecules in the solution.

On the DPDAP bilayer, the condensed DNA molecules are closely packed, in which the interhelical distance can be determined from an average radius of the diffraction ring in the Fourier transform. Figure 4 shows two examples. These results are consistent with our previous findings.⁴⁰ The pitch of DNA can be seen on many segments of DNA in these high-

resolution AFM images, consistent with other results.^{39,40} The average radius of the ring in the Fourier transforms represents the average interhelical distance of the closely packed DNA molecules. The lack of any diffractive spot indicates the absence of any long-range order. When the incubation solution contains DNA at a concentration over 5 $\mu\text{g/mL}$, some segments of DNA are exposed to the solution because of the lack of free membrane surfaces, as shown in Figure 5. These free ends are not stable so that they cause the tip to jump up while scanning across them, resulting in the irregular white spots in the AFM image.

The effect of ionic strength on the condensed DNA on DPDAP has been studied by changing the concentration of NaCl. We have tried to incubate DNA specimens with solutions of high NaCl concentrations for periods over 1.5 h and have found that DNA molecules remained closely packed. It is found that DNA molecules are still condensed onto the cationic bilayer for up to 1 M Na^+ ions. Figure 6 shows two examples, in which part a is an image of DNA incubated in 20 mM NaCl. Note the apparent helical pitch in several DNA segments. The same specimen in part a was then incubated with 200 mM NaCl for a period over 1.5 h at room temperature, washed, and examined with *in situ* AFM. The above procedure was repeated for solutions of 500 mM and 1 M NaCl. A typical AFM image of the same specimen, after the last procedure (incubating with 1 M NaCl), is shown in part b, in which DNA molecules remain condensed. It is interesting that the interhelical distance actually increases at the increase of the salt concentration, as shown by the Fourier transforms of the corresponding AFM images in Figure 6. The relationship of the ionic strength *vs* the

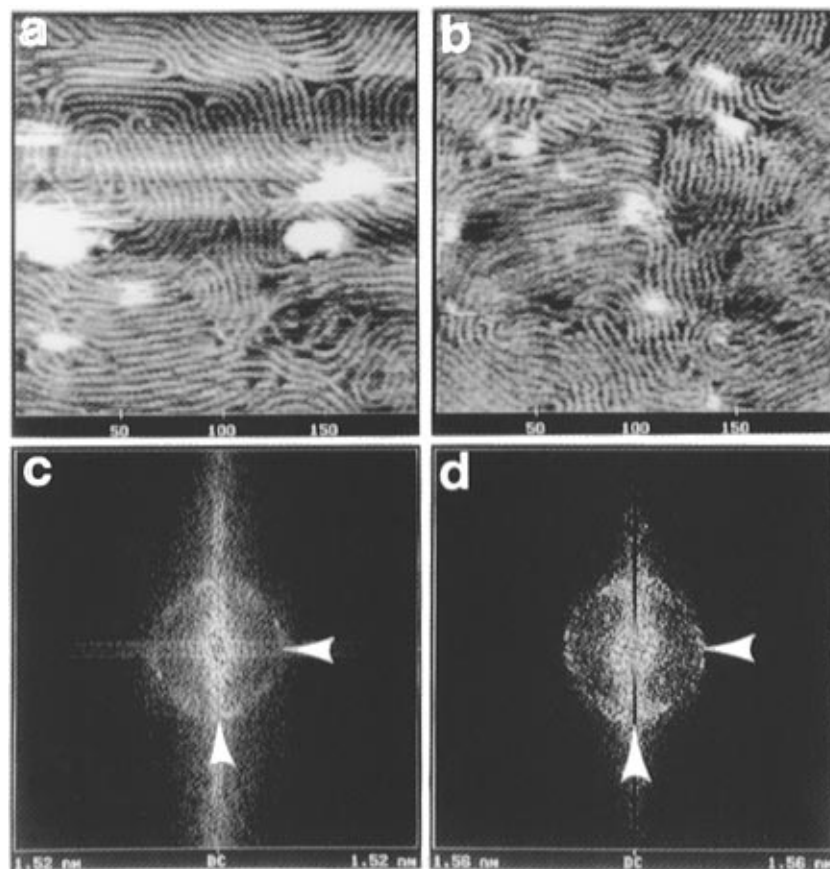


Figure 4. Two typical images of the condensed DNA molecules on DPDAP in 20 mM NaCl and the corresponding Fourier transforms. The image in (a) is the pZT plasmid DNA molecules on DPDAP, and the corresponding Fourier transform is shown in (c). The image in (b) is the marker DNA fragments of pUC 18 Hae III digest on DPDAP, with the corresponding Fourier transform shown in (d). The horizontal arrows in (c) and (d) indicate diffractive spots corresponding to 4.6 and 4.7 nm, and the vertical arrows in (c) and (d) point to those corresponding to 4.4 and 4.5 nm, respectively.

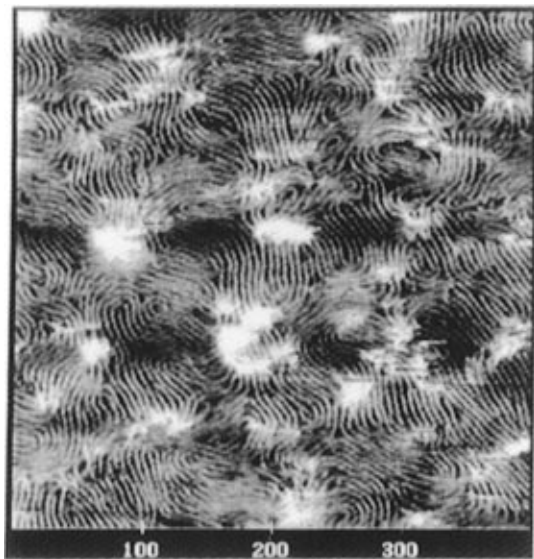


Figure 5. Shown here is an image of closely packed Col E1 plasmid DNA molecules on DPDAP in 20 mM NaCl. There are many bright spots on the image.

interhelical distance is plotted in Figure 6e, in which each datum point is obtained by averaging the radii of the Fourier-transforming rings from about 10 images. A linear dependence is established.

We found that the image contrast reduces drastically at high salt solutions with the DNA specimens. Figure 7 shows an example. Here the image in part a was obtained in 200 mM NaCl, in which some DNA segments were barely visible only in some areas. It is very difficult to obtain an image of good quality while imaging in 200 mM NaCl. However, the image force remains stable without any adhesion force, unlike the case reported elsewhere in which tip contamination causes unstable imaging forces and false images.⁶² The imaging in water improves the situation a lot but still is not totally satisfactory. Closely packed DNA molecules were seen on the same specimen when imaged in water, as shown in Figure 7b. The reason behind this phenomenon is not clear at present.

Condensation of DNA on DSDAP. For the DSDAP, the lipid is in the gel phase and is well below the main phase transition at room temperature. In this case, interhelical distances are larger for DNA molecules adsorbed onto the membrane. Increasing both the incubation time and the DNA concentration at room temperature or 4 °C does not cause any noticeable change in the arrangement of DNA on the membrane. However, the inter helical distance reduces dramatically after heating the membrane to pass through the main phase transition. Figure 8 shows images of pZT plasmid DNA molecules and λ -DNA molecules under different conditions. For both specimens, when the DNA molecules were allowed to bind to the DSDAP membrane at room temperature and 4 °C, the adsorbed DNA molecules are relatively widely distributed, as shown in

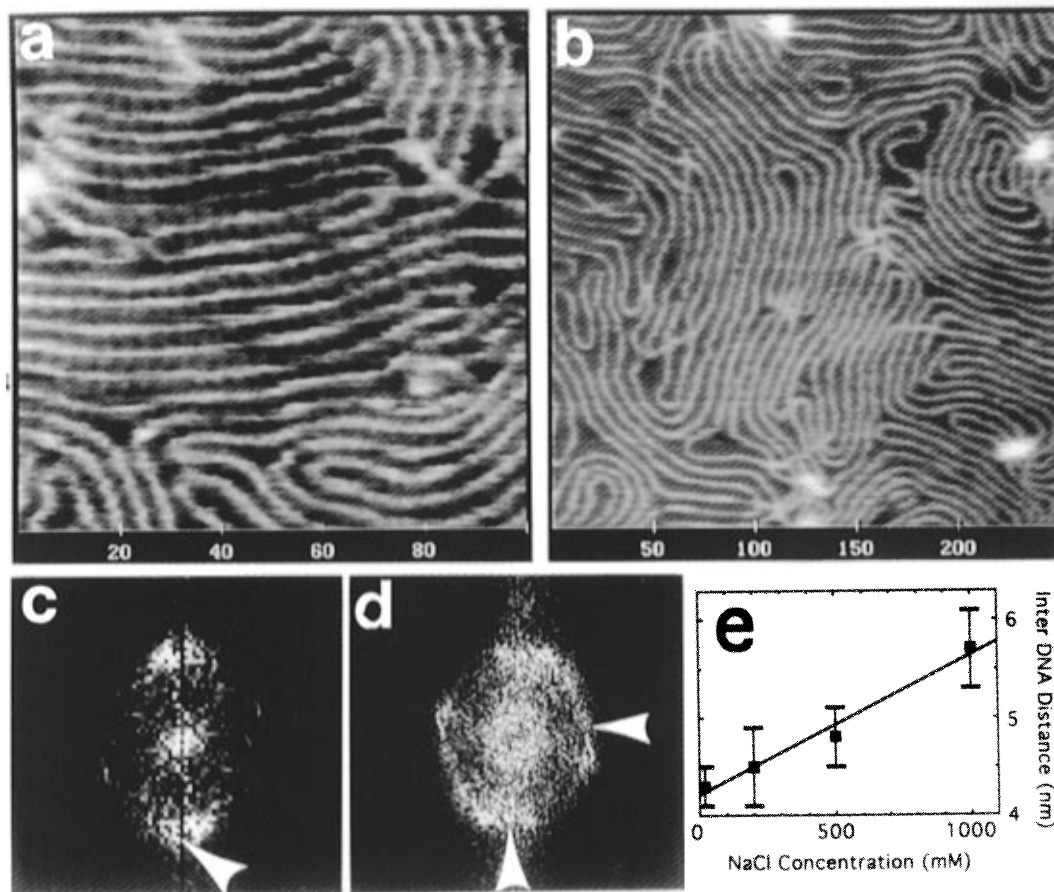


Figure 6. Effect of NaCl concentrations on the interhelical distances. In (a), a typical image of closely packed pZT plasmid DNA molecules on DPDAP in 20 mM NaCl is shown. The Fourier transform of (a) is shown in (c), in which the arrow points to a 4.6 nm spot. The specimen, with which the image in the (a) was obtained, was then treated by incubating with NaCl at different concentrations (200 mM, 500 mM, and 1 M) for over 1½ h each. After each treatment, the specimen was washed with 20 mM NaCl and imaged again in 20 mM NaCl. In (b), we show a typical image of the same specimen in (a) after the last treatment. The Fourier transform of (b) is shown in (d), in which the horizontal arrow points to a 6.7 nm spot and the vertical arrow points to a 6.1 nm spot. In (e), we summarize our studies of the effect due to NaCl concentrations. Each point in (e) corresponds to an average of about 10 images, with the inter helical distance obtained from the average radius of the ring in the Fourier transforms.

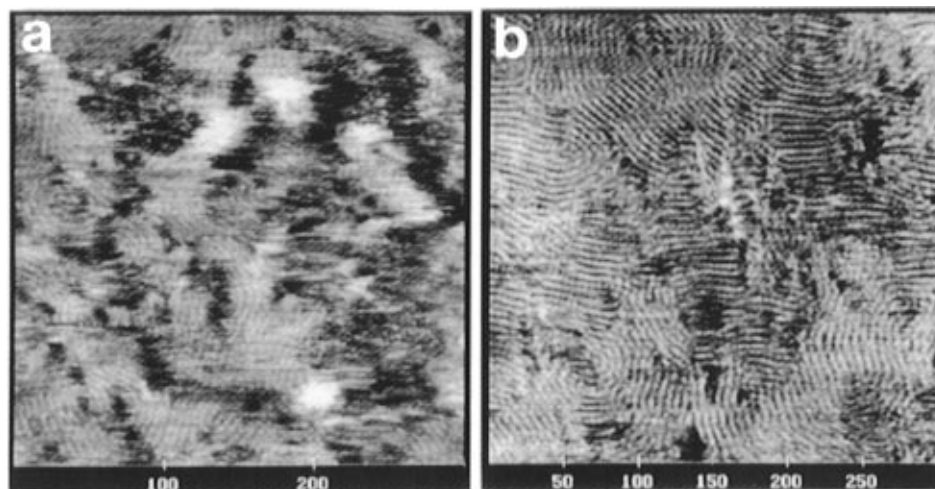


Figure 7. Effect of NaCl concentration on the image quality. The image in (a) was obtained in 200 mM NaCl, and the image in (b) was obtained in distilled and deionized water.

parts a, c, and d. For the plasmid DNA specimen, stable imaging at room temperature was very difficult, although the force curve was steady without any adhesion force. Thus, the image was obtained at lower temperature ($\sim 9^\circ\text{C}$) to improve the situation and to facilitate stable imaging of the widely distributed plasmid DNA on DSDAP membrane. For the λ -DNA specimen, imaging at room temperature was not as difficult, demonstrated by the possibility of visualizing DNA strands at the minimal imaging force (~ 0.1 nN). The height of the widely distributed plasmid DNA is 2.0 ± 0.2 nm (36 measurements) and that of the widely distributed λ -DNA is 2.5 ± 0.5 nm (33 measurements), indicating the absence of any vertical compression by the tip and consistent with other reports.³⁹ The full widths at half-height are 5.8 ± 1.6 nm for the plasmid DNA and 9.5 ± 2.8 nm for the λ -DNA, demonstrating the existence of tip broadening. The height-measurements are in sharp contrast to those of imaging DNA in air or in organic solvents, in which the height of DNA is much lower, while the lateral dimension is consistent with those cases.^{63–70} The larger full width at half-height for the λ -DNA may arise from some tip-induced movements of the DNA as the tip scanned across the DNA.

After obtaining the AFM images, the specimens in parts a, c, and d were heated to 45°C for about 40 min, in the absence of any free DNA molecule in 20 mM NaCl. These treatments cause the bilayer to pass through the main phase transition, so that the lipid molecules in the bilayer are in the fluid phase for the same length of period before cooling back to room temperature. Parts b, e, and f of Figure 8 are the same specimens in parts a, c, and d, respectively. Thus, DNA molecules tend to come closer together on the fluid phase bilayer. The interhelical distances apparently reduce, resulting in the formation of closely packed DNA patches on the membrane. These phenomena suggest the existence of an attraction between DNA helices while they are on fluid phase membranes. For the λ -DNA specimen, we did not observe the small patches as those for the pZT plasmid specimen. However, we did see boundaries after the heating (data not shown). This phenomenon may be due to the much larger size of the λ -DNA and the limited scanning window in the AFM. The DNA molecules in these images are of relatively large molecular size, with the pZT plasmid of 2880 bp and the λ -DNA of 48 kbp. Further, the plasmid is a circular DNA that under normal conditions has some degrees of writhe and is thus supercoiled. Thus, the close packing may also be partially facilitated by some entropic topological constraints from these large DNA molecules

after the dimensionality reduction by condensing onto the 2-D membrane. Under these circumstances, we would expect a slightly different behavior for short DNA molecules. This is indeed the case.

Figure 9 shows a pair of images of short DNA fragments on the same DSDAP bilayer. In part a, the incubation was carried out at room temperature and 4°C over a long period. Thus, the observed wide distribution of DNA is consistent with the results described in the above. However, the same specimen, after incubating at 45°C for about 40 min in DNA-free solution (20 mM NaCl) did not show any apparent change in the DNA arrangement on the membrane. The close packing of the short DNA molecules occurred only after coincubating the specimen with $1\ \mu\text{g/mL}$ DNA at 45°C for about 40 min, as shown in Figure 9b. The formation of the closely packed DNA indicates that more DNA molecules from the solution are bound to the membrane. Thus, although the fluidity of the DSDAP membrane is essential for DNA to be closely packed, the driving force may not be the result of single interacting force among the condensed DNA molecules. It is possible that several factors play roles in the attraction of DNA strands on the membrane, including the phase states of the membrane and the mechanical properties of the polymeric DNA molecules.

Similarly, for both the plasmid DNA and the λ -DNA, the close packing also dominates after incubating the DNA with DSDAP bilayer membranes at 45°C . Figure 10 shows two examples. Here, both kinds of DNA molecules are more closely packed than the examples shown in Figure 9b,e,f. In particular, for the λ -DNA, there are always some free membrane surfaces without any DNA between patches of closely packed DNA. The λ -DNA requires a larger surface area to fully condense onto the 2-D membrane because of its relatively larger size. Thus, if the close packing of λ -DNA results in some free membrane surfaces which are not large enough to accommodate single λ -DNA molecule, these surfaces may remain free.

Discussion

Many biological activities involving DNA require close contacts of DNA helices *in vivo*, and some specific samples are quoted in the Introduction. The condensation of DNA in cellular systems has also been studied.⁷¹ Medical applications in gene therapy also involve close spatial association of DNA strands for expression.⁷² The study of the condensation of DNA may provide clues about factors which play important roles in facilitating the proximity of DNA under various conditions.^{17,71}

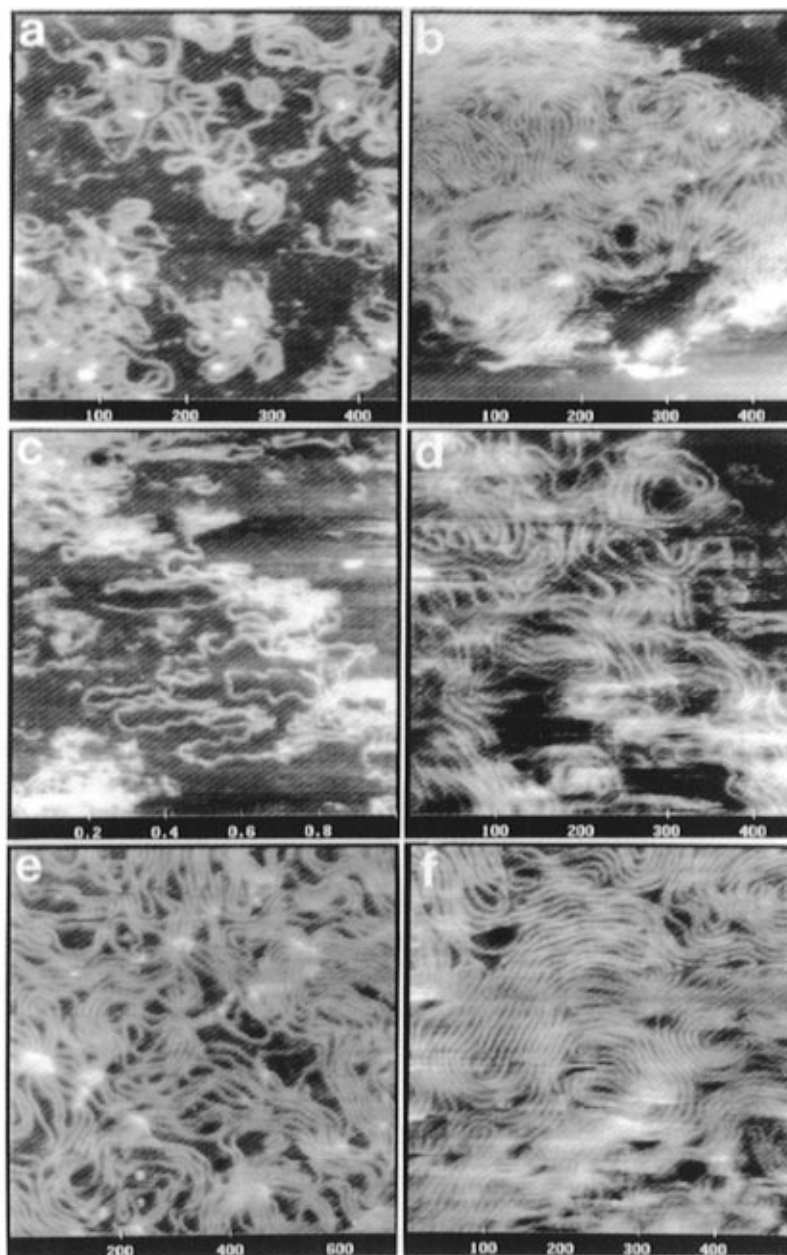


Figure 8. Several images of DNA molecules on DSDAP bilayers in 20 mM NaCl. The image in (a) was taken at 9 °C of pZT plasmid DNA. The same specimen, after heating to 45 °C for 30 min, shows the appearance of patches of much closely packed DNA. A typical example is shown in (b). Two widely distributed examples of λ -DNA are shown in (c) and (d), in which λ -DNA molecules were incubated with a DSDAP bilayer at room temperature for several hours and at 4 °C overnight. For the same specimen, after heating to 45 °C about 30 min, the inter helical distance also decreases, as shown in (e) and (f).

Our results in the condensation of DNA accompanying the dimensionality reduction may provide information about some structural characteristics in the use of cationic liposomes as gene delivery means.^{73–75} Examining structural features of the condensed DNA molecules under various conditions may also provide clues to understand the DNA–DNA interaction on the cationic membranes. There may exist agents or components which act similarly as the cationic lipids to facilitate the proximity of DNA strands in living organisms.

The condensation of adsorbed DNA is independent of the length of DNA. Further, the closely packed DNA lacks any long-range order. In our experiments, it requires the presence of more free DNA molecules in the solution for the DNA condensation on the cationic membranes to occur. The ratio of the condensed DNA to the total DNA available is about 5%. When the concentration of DNA in the incubation is less than 1 $\mu\text{g/mL}$, the adsorbed DNA must be not condensed during

the incubation period (overnight), evidenced by the fact of being unable to obtain stable AFM images. However, longer incubation time also resulted in the condensation in several occasions (approximately several days for 0.2 $\mu\text{g/mL}$, data not shown). After the condensation, washing away excess DNA molecules in the solution did not cause the exit of the condensed DNA, indicating an asymmetric behavior of the DNA molecules in binding and leaving the membrane. This phenomenon distinguishes the condensation in our system from those in the 3-D environment in which DNA molecules condense into structurally well-defined toroids or rods in the presence of polyvalent cations.^{17,21,25}

To understand the mechanism behind the 2-D condensation phenomenon in our systems, we need to examine the substrates, the supported membranes of DPDAP and DSDAP. The phase behaviors of the two lipids are somewhat different. The DPDAP has a rather broad transition peak, indicating the existence of

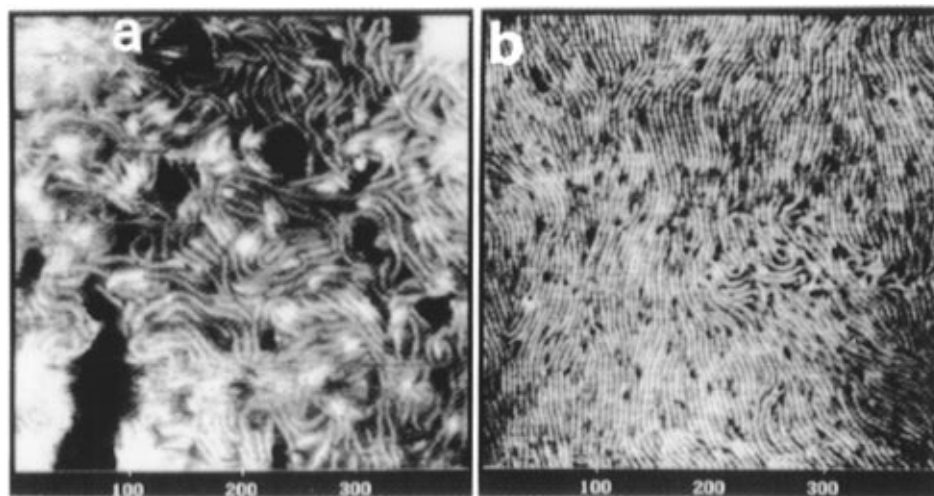


Figure 9. Two images of the DNA fragments on the same DSDAP bilayer in 20 mM NaCl. Initially, the DSDAP bilayer was incubated with DNA at room temperature and at 4 °C, with a total incubation time over 14 h. This procedure did not result in the closely packed DNA on the membrane, as shown in (a). The same specimen, after being heated to 45 °C in the presence of about 1 $\mu\text{g/mL}$ DNA for about 30 min, the close packing of DNA dominates, as shown in (b).

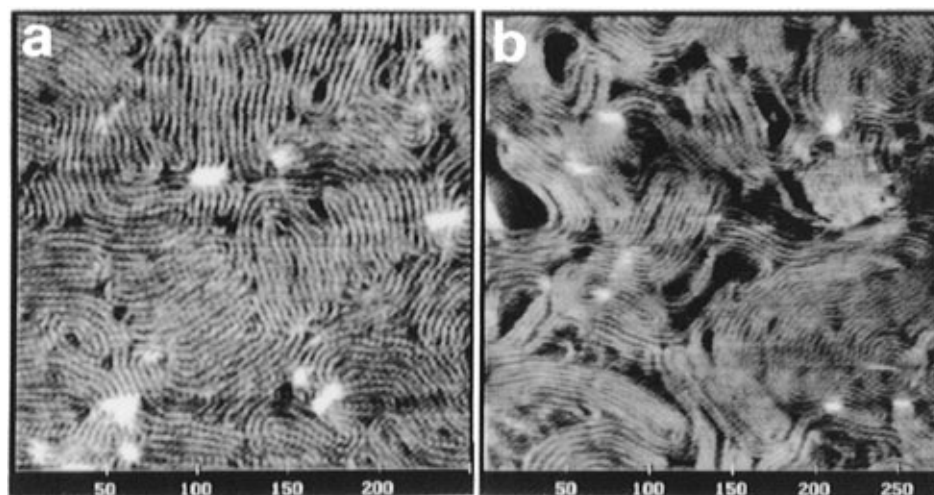


Figure 10. Two typical images of DNA on DSDAP in 20 mM NaCl while the DNA adsorption incubation was carried out at 45 °C for 30 min. The image in (a) shows pZT plasmids, and that in (b) shows λ -DNA molecules.

some metastable states.⁷⁶ The DSDAP has a sharp transition, similar to the typical phase characteristic of phospholipids.^{59,77} The transition enthalpies of the two cationic lipids are considerably higher than those in the phospholipids. The difference in the transition enthalpies between DPDAP and DSDAP, however, is consistent with the acyl chain length increase of the latter.^{59,77} Thus, if the transition enthalpies of the main phase transition in phospholipids are mainly the melting of hydrophobic acyl chains, the larger transition enthalpies of the cationic lipids are likely a result of electrostatic interactions among the charged headgroups.

The experiments with DSDAP bilayers show a strong dependence of the close packing of DNA on the lipid fluidity, suggesting that the diffusive movements of lipids facilitate the close packing, although other factors may also play roles. We present two possible situations in Figure 11 to model the DNA–membrane system. In Figure 11a, the section of a negatively charged rod that represents a DNA segment is placed on top of the positively charged membrane surface. The segment sees a positively charged sea without *a priori* location of any potential well. Then, the segment should see the same positively charged sea whether the lipids are in the fluid phase or in the gel phase. If this is the case, the close packing should be due to some kind of DNA–DNA interaction while on top of the positively

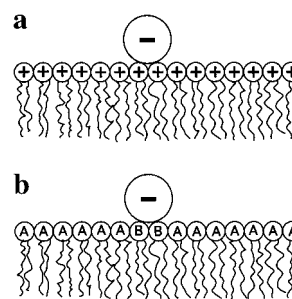


Figure 11. Two illustrations model the DNA cationic membrane system. In (a), a DNA molecule sees the positively charged bilayer sea. In (b), there are two kinds of lipid molecules in the bilayer, with A-type as free lipids and B-type as those that bind to DNA.

charged sea. Then, the observed close packing might be due to an increase in temperature rather than any dependence on the phase behavior of the substrate membrane. However, for any temperature dependence, we would expect the opposite that at higher temperatures DNA should tend to widely distributed, because of the increasing thermal fluctuations. Thus such a model would draw a conclusion inconsistent with our results.

The model in Figure 11b indicates that those lipids which bind to the charged rod are different from those lipids which are free in the bilayer. Then, there are two kinds of positively

charged lipids in the bilayer, with A-type just the normal lipids in the bilayer and B-type that binds to the charged rod. The complex of the negatively charged DNA with the B-type lipids may have an overall new charge which is likely to be negative because of the high charge density of the "DNA rod". It is possible that mixing is favored in such a system containing the complexes and the A-type lipids, according to a theoretical analysis.⁷⁸ Thus, the fluidity of the lipids is essential to allow the "DNA rods" to move closer under the influence of the "mixing".

A more sophisticated model has recently been proposed by Dan that may explain the essential mechanism involved in our experiments.⁷⁹ According to the theory, the binding of a uniformly charged rod causes lipids in the fluid-phase bilayer around the rod to creep up at the sides of the rod. This thickness increase at the vicinity of two rods pulls them together due to the hydrophobic mismatch. The theory predicts two types of condensed phases, depending on a membrane-DNA coupling constant and various other environmental factors, such as ionic strength, the structure of lipids in the membrane, and mechanical properties of the membrane. The coupling constant and the mechanical properties of the membrane are difficult to measure experimentally. In one type of the condensed phase, a relative thickness difference of about 3% would result in an interrod distance of about 5 nm, assuming the rod itself is flexible on the membrane, in striking agreement with our experimental results. For the gel-phase lipids, a strong chain-chain interaction prevents the creeping, and thus, the hydrophobic mismatch induced attraction between the rods is absent. Moreover, with gel-phase lipids, the very restricted diffusion of the lipids also impedes any spatial rearrangement once DNA molecules adsorbed to the membrane, preventing any close packing of the DNA. For short DNA fragments, the stiffness of the DNA may overcome any attraction so that DNA molecules remain widely distributed after heating the membrane to pass the main phase transition temperature. This phenomenon indicates that the energetics of the DNA-DNA interaction involves delicate interplay and balance among various forces and a slight variation of one or the other may determine the overall outcome. This case is similar to the DNA condensation induced by polyvalent cations in 3-D, in which the net interaction per base pair is of order 10^{-2} – 10^{-3} kT , with kT the thermal energy at room temperature.¹⁷

If during incubation the lipids are in the fluid phase, an additional force also exists to push DNA molecules close together as more DNA molecules in solution are trying to bind to the membrane. This additional force may be sufficient to overcome the stiffness of short DNA fragments so that the close packing of DNA molecules is favorable, as shown in Figure 9b. For the case with DPDAP, the broad main phase transition indicates that the lipids may still retain some fluidity in the presence of some metastable states at temperatures not too low below the transition temperature. The additional force from binding of free DNA molecules to the membrane is always available in the binding of DNA to DPDAP. Therefore, Dan's theory may still be valid, consistent again with our experiments.

In order to analyze the effect of Na^+ ions on the behavior of the condensed DNA in the 2-D systems, we can imagine the positively charged bilayer as a giant polyvalent cation substrate. Then, the presence of monovalent Na^+ ions competes with the substrate to weaken the binding of DNA to the substrate. Our experiments indicate that the membrane-DNA attraction must be very strong so that DNA molecules remain bound to the membrane even for 1 M Na^+ ions. The geometry of the 2-D system containing the condensed DNA shows that most surfaces

of the "DNA rod" are exposed to the solution. This is due to the fact the DNA is known to have an average radius of 2 nm, and the interhelical distances in our systems are larger than 4 nm. On these exposed surfaces, there are nonlocalized Na^+ ions condensed onto the "DNA rod" according to Manning's theory.³⁰ We can imagine that these nonlocalized Na^+ ions actually increase the effective radius of the "DNA rod". At higher Na^+ concentration, the "DNA rod" becomes larger at the condensation of more Na^+ ions. Thus, the interhelical distances increase at higher Na^+ concentrations.

In the contact-mode AFM, the resolution of two objects in close vicinity requires a detectable force difference between the tip on top of the objects and the tip on top of the space between them. If there is a layer of some substances screening the tip-sample interaction, the force-difference signal corresponding to the contrast decreases. When the screening becomes severe, it is possible to lose the resolution of the two objects. Thus, the facts that we did not obtain stable AFM image at high Na^+ concentration and were able to image the same specimen in water or in a low Na^+ concentration solution mean that there exist some screening layers between the 2-D system and the AFM tip at high Na^+ concentrations. The major physical character at higher Na^+ concentrations in our system should be the condensation of more nonlocalized Na^+ ions onto available surfaces of membrane-adsorbed DNA molecules. Thus, it appears that those nonlocalized Na^+ form a screening layer between the DNA on the membrane and the AFM tip. In reality, a hydration layer should enclose the surface of all entities of interest here.^{80,81} The effective screening layer should include the hydration layer. It appears that our crude analysis may paint an intuitive physical picture of the Na^+ effect observed here, although detailed theoretical analyses are needed to fully understand the phenomenon. Some studies of other systems may also help future theoretical analyses. For DNA molecules in salt solutions, the repulsion between DNA decreases as the concentration of NaCl increases.⁸² The condensation of DNA into toroids induced by polyvalent cations requires higher polycation concentration at higher NaCl concentration.^{27,28} These results, to a first-order approximation, are consistent with the screening effect by the binding of Na^+ ions to DNA, as predicted in Manning's theory.³⁰ A more detailed analysis by Rau and Parsegian shows that the osmotic pressure is dominated by a hydration force in the DNA-DNA interaction, in salt solutions at short interhelical distances (<4 nm).⁸³

In summary, we have shown that *in situ* atomic-force microscopy facilitates structural studies of the 2-D condensation of DNA onto cationic lipid membranes. The fluidity of the cationic membrane promotes the close packing of the condensed DNA molecules, independent of the length of the DNA and disregarding whether the DNA molecule is linear or circular. The average interhelical distance for closely packed DNA is over twice the average diameter of DNA. This study also demonstrates the usefulness of the newly developed AFM in structural biology and indicates that even higher spatial resolution is possible with further development.

Acknowledgment. We are grateful to N. Dan, R. Bansil, and K. A. Marx for many helpful discussions. We are also grateful to N. Dan for sending us a manuscript prior to its publication. We appreciate helpful suggestions from two anonymous reviewers. Support from the U.S. Army Research Office and the American Heart Association Vermont Affiliated Grant in Add is acknowledged.

References and Notes

- (1) Camerini-Otero, R. D.; Hsieh, P. *Cell* **1993**, *73*, 217.

- (2) Kleckner, N.; Weiner, B. M. *Cold Spring Harbor Symp. Quant. Biol.* **1993**, 58, 553.
- (3) Menetski, J. P.; Bear, D. G.; Kowalczykowski, S. C. *Proc. Natl. Acad. Sci. U.S.A.* **1990**, 87, 21.
- (4) Sikorav, J.-L.; Church, G. M. *J. Mol. Biol.* **1991**, 222, 1085.
- (5) Pfeiffer, B. H.; Zimmerman, S. B. *Nucl. Acids Res.* **1983**, 11, 7853.
- (6) Zimmerman, S. B.; Harrison, B. *Proc. Natl. Acad. Sci. U.S.A.* **1987**, 84, 1871.
- (7) Krasnow, M. A.; Cozzarelli, N. R. *J. Biol. Chem.* **1982**, 257, 2687.
- (8) Fuller, R. S.; Kauni, J. M.; Kornberg, A. *Proc. Natl. Acad. Sci. U.S.A.* **1981**, 78, 7370.
- (9) Kornberg, A.; Baker, T. A. *DNA Replication*, 2nd ed.; W. H. Freeman: New York, 1992.
- (10) Tsurimoto, T.; Matsubara, K. *Biochemistry* **1982**, 79, 7639.
- (11) Leforestier, A.; Livolant, F. *Biophys. J.* **1994**, 65, 56.
- (12) Livolant, F. *Physica A* **1991**, 176, 117.
- (13) Rill, R. L.; Strzelecka, T. E.; Davidson, M. W.; van Winke, D. H. *Physica A* **1991**, 176, 87.
- (14) Podgornik, R.; Strey, H. H.; Gawrisch, K.; Rau, D. C.; Rupprecht, A.; Parsegian, V. A. *Proc. Natl. Acad. Sci. U.S.A.* **1996**, 93, 4261.
- (15) Sikorav, J. L.; Pelta, J.; Livolant, F. *Biophys. J.* **1994**, 67, 1387.
- (16) Baeza, I.; Gariglio, P.; Rangel, L. M.; Chavez, P.; Cervants, L.; Arguello, C.; Wong, C.; Montanez, C. *Biochemistry* **1987**, 26, 6387.
- (17) Bloomfield, V. A. *Biopolymers* **1991**, 31, 1471.
- (18) Chattoraj, D. K.; Gosule, L. C.; Schellman, J. A. *J. Mol. Biol.* **1978**, 121, 327.
- (19) Gosule, L. C.; Schellman, J. A. *Nature* **1976**, 259, 333.
- (20) Ma, C.; Bloomfield, V. A. *Biophys. J.* **1994**, 67, 1678.
- (21) Manning, G. S. *Cell Biophys.* **1985**, 7, 57.
- (22) Marquet, R.; Houssier, C. *J. Biomol. Struct. Dyn.* **1991**, 9, 159.
- (23) Marx, K. A.; Reynolds, T. C. *Proc. Natl. Acad. Sci. U.S.A.* **1982**, 79, 6484.
- (24) Marx, K. A.; Reynolds, T. C. *Int. J. Biol. Macromol.* **1989**, 11, 241.
- (25) Marx, K. A.; Ruben, G. C. *J. Biomol. Struct. Dyn.* **1984**, 1, 1109.
- (26) Schellman, J. A.; Parthasarathy, N. J. *Mol. Biol.* **1984**, 175, 313.
- (27) Widom, J.; Baldwin, R. L. *Biopolymers* **1983**, 22, 1595.
- (28) Widom, J.; Baldwin, R. L. *J. Mol. Biol.* **1980**, 144, 431.
- (29) Wilson, R. W.; Bloomfield, V. A. *Biochemistry* **1979**, 18, 2192.
- (30) Manning, G. S. *Q. Rev. Biophys.* **1978**, 2, 179.
- (31) Binnig, G.; Quate, C. F.; Gerber, C. H. *Phys. Rev. Lett.* **1986**, 56, 930.
- (32) Bustamante, C.; Erie, D.; Keller, D. *Curr. Opin. Struct. Biol.* **1994**, 4, 750.
- (33) Drake, B.; Prater, C. B.; Weisenhorn, A. L.; Gould, S. A. C.; Albrecht, T. R.; Quate, C. F.; Cannell, D. S.; Hansma, H. G.; Hansma, P. K. *Science* **1989**, 243, 1586.
- (34) Hansma, H. G.; Hoh, J. *Annu. Rev. Biophys. Biomol. Struct.* **1994**, 23, 115.
- (35) Lindsay, S. M.; Tao, N. J.; DeRose, J. A.; Oden, P. I.; Lyubchenko, Y. L.; Harrington, R. E.; Shlyakhtenko, L. *Biophys. J.* **1992**, 61, 1570.
- (36) Shao, Z.; Yang, J. *Quart. Rev. Biophys.* **1995**, 28, 195.
- (37) Yang, J.; Shao, Z. *Micron* **1995**, 26, 35.
- (38) Yang, J.; Tamm, L. K.; Somlyo, A. P.; Shao, Z. *J. Microsc.* **1993**, 171, 183.
- (39) Mou, J.; Czajkowsky, D. M.; Zhang, Y.; Shao, Z. *FEBS Lett.* **1995**, 371, 279.
- (40) Yang, J.; Wang, L.; Camerini-Otero, R. D. *Nanobiology*, in press.
- (41) Butt, H.-J.; Downing, K. H.; Hansma, P. K. *Biophys. J.* **1990**, 58, 1473.
- (42) Hoh, J. H.; Sosinsky, G. E.; Revel, J.-P.; Hansma, P. K. *Biophys. J.* **1993**, 65, 149.
- (43) Karrasch, S.; Hegerl, R.; Hoh, J. H.; Baumeister, W.; Engel, A. *Proc. Nat. Acad. Sci. U.S.A.* **1994**, 91, 836.
- (44) Mou, J.; Yang, J.; Shao, Z. *J. Mol. Biol.* **1995**, 248, 507.
- (45) Schabert, F. A.; Henn, C.; Engel, A. *Science* **1995**, 268, 92.
- (46) Yang, J.; Tamm, L. K.; Tillack, T. W.; Shao, Z. *J. Mol. Biol.* **1993**, 229, 286.
- (47) Yang, J.; Mou, J.; Shao, Z. *FEBS Lett.* **1994**, 338, 89.
- (48) Fang, Y.; Yang, J. *J. Phys. Chem.* **1996**, 100, 15614.
- (49) Hui, S. W.; Viswanathan, R.; Zasadzinski, J. N. A.; Israelachvili, J. N. *Biophys. J.* **1995**, 68, 171.
- (50) Mou, J.; Yang, J.; Shao, Z. *Biochemistry* **1994**, 33, 4439.
- (51) Weisenhorn, A. L.; Egger, M.; Ohnesorge, F.; Gould, S. A. C.; Heyn, S.-P.; Hansma, H. G.; Sinsheimer, R. L.; Gaub, H. E.; Hansma, P. K. *Langmuir* **1991**, 7, 8.
- (52) Zasadzinski, J. A. N.; Helm, C. A.; Longo, M. L.; Weisenhorn, A. L.; Gould, S. A. C.; Hansma, P. K. *Biophys. J.* **1991**, 59, 755.
- (53) Boni, L. T.; Minchey, S. R.; Perkins, W. R.; Ahl, P. L.; Slater, J. L.; Tate, M. W.; Gruner, S. M.; Janoff, A. S. *Biochim. Biophys. Acta* **1993**, 1146, 247.
- (54) Kantor, H. L.; Mabrey, S.; Prestegard, J. H.; Sturtevant, J. M. *Biochim. Biophys. Acta* **1977**, 466, 402.
- (55) Felgner, P. L.; Gadek, T. R.; Holm, M.; Roman, R.; Chan, H. W.; Wenz, M.; Northrop, J. P.; Ringold, G. M.; Danielsen, M. *Proc. Natl. Acad. Sci. U.S.A.* **1987**, 84, 7413.
- (56) Stamatis, L.; Leventis, R.; Zuckermann, M. J.; Silviu, J. R. *Biochemistry* **1988**, 27, 3917.
- (57) Bayerl, T. M.; Bloom, M. *Biophys. J.* **1990**, 58, 357.
- (58) Johnson, S. J.; Bayerl, T. M.; McDermott, D. C.; Adam, G. W.; Rennie, A. R.; Thomas, R. K.; Sackmann, E. *Biophys. J.* **1991**, 59, 289.
- (59) Cevc, G.; Marsh, D. *Phospholipid Bilayers: Physical Properties and Model*; Wiley: New York, 1987.
- (60) Nagle, J. F. *Faraday Discuss. Chem. Soc.* **1986**, 81, 151.
- (61) Richmond, G. L. In *Electrochemical Interfaces: Modern Techniques for in-Situ Interface Characterization*; Abruna, H. D., Ed.; VCH Publishers: New York, 1991; pp 265–337.
- (62) Yang, J.; Mou, J.; Shao, Z. *Biochim. Biophys. Acta* **1994**, 1199, 105.
- (63) Bustamante, C.; Vesenska, J.; Tang, C. L.; Rees, W.; Guthod M.; Keller, R. *Biochemistry* **1992**, 31, 22.
- (64) Hansma, H. G.; Vesenska, J.; Siegerist, C.; Kelderman, G.; Morrett, H.; Sinsheimer, R. L.; Elings, V.; Bustamante C.; Hansma, P. K. *Science* **1992**, 256, 1180.
- (65) Hansma, H. G.; Sinsheimer, R. L.; Groppe, J.; Bruice, T. C.; Elings, V.; Gurley, G.; Bezanilla, M.; Mastrangelo, I. A.; Hough, P. V. C.; Hansma, P. K. *Scanning* **1993**, 15, 296.
- (66) Hansma, H. G.; Browne, K. A.; Bezanilla, M.; Bruice, T. C. *Biochemistry* **1994**, 33, 8436.
- (67) Lyubchenko, Y. L.; Oden, P. I.; Lampner, D.; Lindsay S. M.; Dunker, K. A. *Nucl. Acids Res.* **1993**, 21, 1117.
- (68) Shaiu, W.-L.; Larson, D. D.; Vesenska, J.; Henderson, E. *Nucl. Acids Res.* **1993**, 21, 99.
- (69) Yang, J.; Shao, Z. *Ultramicroscopy* **1993**, 50, 157.
- (70) Yang, J.; Takeyasu K.; Shao, Z. *FEBS Lett.* **1992**, 301, 173.
- (71) Kellenberger, E. *Biophys. Chem.* **1988**, 29, 51.
- (72) Zhu, N.; Liggitt, D.; Liu, Y.; Debs, R. *Science* **1993**, 261, 209.
- (73) Wong, F. M. P.; Reimer, D.; Bally, M. B. *Biochemistry* **1996**, 35, 5756.
- (74) Xu, Y.; Szoka, Jr., F. C. *Biochemistry* **1996**, 35, 5616.
- (75) Lasic, D. D.; Strey, H.; Podgornik, R.; Frederik, P. M. 4th European Symposium on Controlled Drug Delivery, The Netherlands, 1996; p 61.
- (76) Suurkuusk, J.; Lentz, B. R.; Barenholz, Y.; Biltonen, R. L.; Thompson, T. E. *Biochemistry* **1976**, 15, 1393.
- (77) Nagle, J. F. *Annu. Rev. Phys. Chem.* **1980**, 31, 157.
- (78) MacKintosh, F. C.; Safran, S. A. *Phys. Rev. E* **1993**, 47, 1180.
- (79) Dan, N. *Biophys. J.* **1996**, 71, 1267.
- (80) Leikin, S.; Parsegian, V. A.; Rau, D. C.; Rand, R. P. *Annu. Rev. Phys. Chem.* **1993**, 44, 369.
- (81) Israelachvili, J.; Wennerström, H. *Nature* **1996**, 379, 219.
- (82) Podgornik, R.; Rau, D. C.; Parsegian, V. A. *Biophys. J.* **1994**, 66, 962.
- (83) Rau, D. C.; Parsegian, V. A. *Biophys. J.* **1992**, 61, 246.